Exact Solution to the One-Dimensional Inverse-Stefan Problem in Nonideal Biological Tissues

Y. Rabin

A. Shitzer

Department of Mechanical Engineering,
Technion - Israel Institute of Technology,
Haifa 32000, Israel

A new analytic solution of the inverse-Stefan problem in biological tissues is presented. The solution, which is based on the enthalpy method, assumes that phase change occurs over a temperature range and includes the thermal effects of metabolic heat generation, blood perfusion, and density changes. As a first stage a quasi-steady-state solution is derived, defined by uniform velocities of the freezing fronts and thus by constant cooling rates at those interfaces. Next, the fixed boundary condition leading to the quasi-steady state is calculated. It is shown that the inverse-Stefan problem may not be solved exactly for a uniform initial condition, but rather for a very closely approximating exponential initial condition. Very good agreement is obtained between the new solution and an earlier one assuming biological tissues to behave as pure materials in which phase change occurs at a single temperature. A parametric study of the new solution is presented taking into account property values of biological tissues at low freezing rates typical of cryosurgical treatments.

Introduction

The freezing response of most biological tissues can be generalized by a theory known as the "two-factor hypothesis" of freezing damage (Mazur et al., 1972). The recovery of frozen biological tissue reveals an optimum cooling rate, which suggests this hypothesis. Tissue destruction at low cooling rates is linked to the "solution effect" whereas tissue destruction at high cooling rates is linked to the formation of intracellular ice (Mazur, 1963; Fahy, 1981; McGrath 1993). It is generally accepted that at those widely different cooling rates maximal destruction of biological tissues is achievable (Farrant, 1971; Akhtar et al., 1979; Gage et al., 1985; Miller and Mazur, 1976; Augustynowicz and Gage, 1985). These cooling rates, of the order of a few or hundreds of degrees Centigrade per minute, respectively, may vary among different tissues (Rubinsky and Onik, 1991).

Freezing at low cooling rates is better suited for cryosurgical applications as it allows deeper penetration of the cryotreatment. Therefore, one of the most important criteria for the success of a cryosurgical treatment is the maintenance of a desired low cooling rate at the freezing front during phase change (Orpwood, 1981).

In typical cryosurgical processes, the cooling rates vary throughout the tissue. An appropriate analysis of this problem, termed the Stefan problem, would facilitate the prediction of these variable cooling rates, and the location of the freezing front, e.g., Carslaw and Jaeger (1959). In these processes the variation of the temperature forcing function as effected by the cryoprobe, is specified as a boundary condition in the solution.

There also exists another family of solutions for phase change problems known as the inverse-Stefan problems. In this class of problems the desired cooling rate at the freezing front is the required boundary condition, whereas the temperature forcing function, at the interface with the cryoprobe, is calculated by the analysis. In this paper, we address this class of inverse-Stefan problems, namely, calculate the temperature forcing function, which is required to achieve certain desired cooling rates at the phase-change front in the tissue.

Phase change in a biological tissue, which is a nonideal material, occurs over a relatively wide temperature range. The upper limit of this range may be between −0.5°C and −1°C, whereas the lower limit may be between −5°C and −8°C (Altman and Dittmer, 1971; Wessling and Blackshear, 1973). This range of temperatures within which phase transition occurs excludes the application of existing analytic solutions to the inverse-Stefan problems, which assume phase change to occur at a single temperature (Carslaw and Jaeger, 1959; Rubinsky and Shitzer, 1976; Alexiades and Solomon, 1993). The only existing approximate analytic solution by Budman et al. (1993), which treats the biological tissue as a nonideal material, does not include heating due to metabolic processes nor does it account for the effects of blood perfusion. Rubinsky (1989) developed a microscopic scale model describing the relationship between heat and mass transfer and the response of the cells and blood vessels. The analysis is limited to cases without blood perfusion.

This paper presents an exact analytic solution to the inverse-Stefan problem in a biological tissue. The tissue is treated as a nonideal substance, freezing over a range of temperatures, which includes both metabolic heat and blood perfusion effects. The solution presented is based on the enthalpy method, which assumes that the latent heat of solidification is incorporated into the specific heat. Initially, the solution to the quasi-steady-state inverse-Stefan problem is presented. Based on this solution, a boundary condition that yields this quasi-steady state, is calculated.

The solution presented is general and is applicable to nonbiological materials by simply setting metabolic heat and blood perfusion to zero. Applications are numerous, including calculation of optimal cooling rates in food processing, prevention of thermal stresses in metal casting processes, etc.

Problem Definition

The peak phase-change temperature T_{m1} is defined as that at which the specific heat function attains a maximal value, Fig. 1. Enclosing this temperature are two regions undergoing phase transition: region [1] in which the temperature is below the upper limit of the phase-change temperature range, $T_{m1} \leq T \leq T_{ml}$, and

Contributed by the Heat Transfer Division for publication in the JOURNAL OF HEAT TRANSFER. Manuscript received by the Heat Transfer Division November 1993; revision received July 1994. Keywords: Phase-Change Phenomena, Transient and Unsteady Heat Transfer. Associate Technical Editor: R. Viskanta.

region [2] in which the temperature is above the lower limit of the phase-change temperature range, $T_{mf} \leq T \leq T_{m1}$. All in all, we identify four regions in the medium: unfrozen, frozen, and the two regions in the phase transition range. These regions are separated by three freezing fronts, s_f, s_1 and s_l, defined by the isotherms T_{mf}, T_{m1}, and T_{ml}, respectively, Fig. 1.

It is noted that the division of the domain into four regions and the definition of freezing front s_1 is due to mathematical considerations and does not bear any physiological significance. This division facilitates the inclusion of the variations of the thermophysical properties in the solution as assumed in Fig. 1.

The one-dimensional, analytic solution is developed for the following conditions:

(*a*) The thermal conductivity is assumed to behave like a three-step temperature dependent function, Fig. 1. Previous solutions treated this property as a one-step (Rubinsky and Shitzer, 1976) or a two-step function (Budman et al., 1993). The present assumption moderates heat fluxes at the various boundaries and further provides for a more realistic depiction of the realistic conditions.

(*b*) The volumetric specific heat is assumed to vary linearly throughout regions [1] and [2], Fig. 1. According to the enthalpy method, or the "weak solution" (Goodman, 1958; Voller, 1986), the coefficients of the specific heat function in these regions may be calculated by the known peak phase-change temperature and the latent heat.

(*c*) During phase change there is a volume change, while the density is assumed constant in each region. This volume change is included in the volumetric specific heat discussed in section (*b*) above.

(*d*) Blood perfusion in the unfrozen region is constant and uniform. This condition approximates closely peripheral tissues, which are supplied by a dense network of capillaries at relatively low blood perfusion rates.

(*e*) Metabolic heat generation in the unfrozen region is constant and uniform.

(*f*) The tissue is assumed to be depicted by a semi-infinite, thermally homogeneous medium.

(*g*) Initially the temperature is uniform throughout the tissue.

In contrast to the existing analytic solutions of closely related problems (Carslaw and Jaeger, 1959; Rubinsky and Shitzer, 1976; Alexiades and Solomon, 1993; Budman et al., 1995), the quasi-steady-state problem is treated first. Subsequently, a forcing function is calculated at the interface between the tissue and the cryoprobe. A quasi-steady state is defined as a full steady state in a system of coordinates that follows the three freezing fronts, Fig. 2. Thus, at this state all freezing fronts advance at a constant and equal velocity and there is no change in the extent of the frozen region. It follows that in a quasi-steady state the cooling rates at the various freezing fronts are constant but may be different from one front to the other. Moreover, there may be a difference in the cooling rates on either side of any front due to the change in the thermophysical properties.

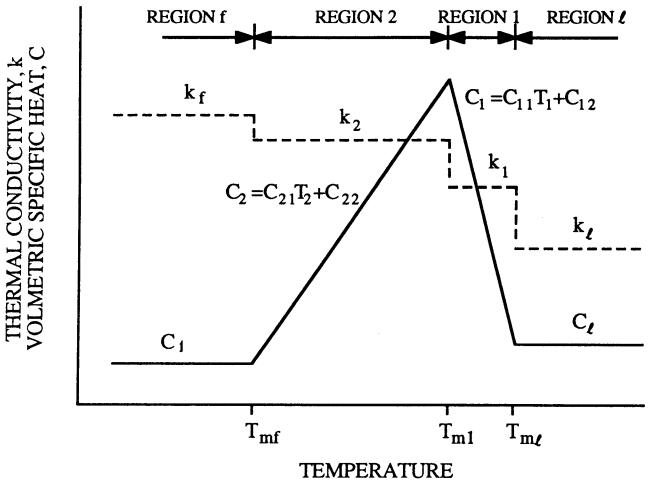

Fig. 1 Schematic presentation of the temperature-dependent thermal conductivity and specific heat functions applied in this study

Analysis

It is customary to assume that in biological tissues characterized by low blood perfusion supplied by a dense capillary network, as is the case for peripheral tissues, the heat balance is given by the classical bioheat equation (Pennes, 1948):

$$C_l \frac{\partial T}{\partial t} = k_l \frac{\partial^2 T}{\partial x^2} + \dot{w}_b C_b (T_b - T) + \dot{q}_{\text{met}} \qquad (1)$$

Nomenclature

a = constant defined in Eqs. (25) and (27) in regions [1] and [2], respectively, 1/m^2
b = constant defined in Eqs. (26) and (28) in regions [1] and [2], respectively, 1/m
C_{ij} = volumetric specific heat coefficients in region i, J/m^3-°C^2 for j = 1 and J/m^3-°C for j = 2
C_l = volumetric specific heat, J/m^3-°C
D = constant of the solution in the unfrozen region, Eq. (3), 1/m
g_{12} = integration constant in Eq. (12), m
g_{11}, g_{21} = integration constants in Eqs. (12) and (15), respectively, 1/m
h = volumetric specific enthalpy, J/m^3
k = thermal conductivity, W/m-°C
L = latent heat, J/m^3
$\dot{q}$ = volumetric heat source, W/m^3
s = interface location, m
t = time, s
T = temperature, °C
$\dot{w}_b$ = volumetric blood perfusion per unit volume of tissue, 1/s
x = coordinate, m
α = thermal diffusivity, m^2/s
ϵ = initial condition parameter defined in Eq. (18)
κ_{ij} = $C_{ij}\dot{s}/k_i$ = ratio of freezing front velocity and thermal diffusivity, defined in Eq. (11), 1/m-°C for j = 1 and 1/m for j = 2
η = transformed coordinate, m
ξ = transformed coordinate, m
τ = time required for freezing front formation, s

Subscripts

0 = initial
1 = of region [1]
2 = of region [2]
$i1$ = slope of a temperature-dependent property in region [i]
$i2$ = constant of a property in region [i]
b = blood
f = frozen
i, j = indices
l = unfrozen
met = metabolic
$m1$ = peak value of specific heat in the phase transition region
mf = lower phase transition temperature boundary
ml = upper phase transition temperature boundary

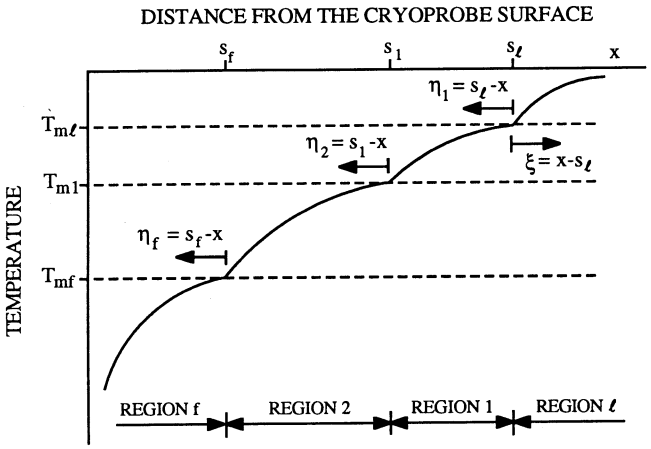

Fig. 2 Schematic presentation of the various coordinate systems tracing the freezing fronts

In the present analysis we distinguish between two main regions in the tissue: frozen and unfrozen. The cooling process in the unfrozen region in a quasi-steady state is well defined mathematically by the temperatures specified on its two boundaries. Thus, the bioheat equation may be solved for this region, independent of the other regions. As suggested by Rubinsky and Shitzer (1976), the temperature distribution in the unfrozen region is given by:

$$T_l = \left(T_b + \frac{\dot{q}_{\text{met}}}{\dot{w}_b C_b}\right)\cdot[1 - \exp(-D\xi)] + T_{ml}\exp(-D\xi) \quad (2)$$

$$D = \frac{\dot{s} + (\dot{s}^2 + 4\dot{w}_b C_b \alpha_l^2/k_l)^{1/2}}{2\alpha_l} \quad (3)$$

Equations (2) and (3) apply to a coordinate system moving with isotherm T_{ml}, Fig. 2. The variable $\dot{s}$ designates the interface velocity, which is identical at all moving fronts in a quasy-steady state.

Once freezing of the tissue is initiated, we assume that both blood perfusion and all metabolic activities cease. This assumption reduces the bioheat equation to a conventional heat diffusion equation, which applies in regions [1], [2], and [f], including the linear dependence of specific heat on the temperature:

$$\frac{C_{i1}T_i + C_{i2}}{k_i}\frac{\partial T_i}{\partial t} = \frac{\partial^2 T_i}{\partial x^2} \quad (4)$$

where the index i can be 1, 2 or f.

Solution of this equation is subject to the following boundary conditions:

$$T_i|_{x=s_j} = T_{mj} \quad (5)$$

$$-k_i \left.\frac{\partial T_i}{\partial x}\right|_{x=s_j}^{+} = -k_j \left.\frac{\partial T_j}{\partial x}\right|_{x=s_j}^{-} \quad (6)$$

where the index i is as in Eq. (4), and the index j relates to regions [l], [1], or [2].

Equations (4)–(6) are transformed to the coordinate systems η_i, to yield:

$$\frac{\partial^2 T_i}{\partial \eta_i^2} = \frac{C_{i1}T_i + C_{i2}}{k_i}\left(\frac{\partial T_i}{\partial t} + \dot{s}\frac{\partial T_i}{\partial \eta_i}\right) \quad (7)$$

$$T_i|_{\eta_i=0} = T_{mi} \quad (8)$$

$$k_i \left.\frac{\partial T_i}{\partial \eta_i}\right|_{\eta_i=0} = \begin{cases} -k_l \left.\dfrac{\partial T_l}{\partial \xi}\right|_{\xi=0} & \text{for} \quad (i=1) \\ k_j \left.\dfrac{\partial T_j}{\partial \eta_j}\right|_{\eta_j=\eta_{sj}} & \text{for} \quad (i=2, j=1) \\ & \text{or} \quad (i=f, j=2) \end{cases} \quad (9)$$

In a quasi-steady state the temperature distribution in the η_i coordinate system is independent of time. Thus, the time derivative in Eq. (7) may be omitted and the partial derivatives may be replaced by ordinary ones to yield:

$$\frac{d^2 T_i}{d\eta_i^2} = (\kappa_{i1}T_i + \kappa_{i2})\frac{dT_i}{d\eta_i} \quad (10)$$

where:

$$\kappa_{ij} \equiv \frac{C_{ij}\dot{s}}{k_i} \quad (11)$$

Equation (10) is integrated in two steps. The first step involves the substitution of the derivative $dT_i/d\eta_i$ by a dummy variable. This yields a first-order differential equation the solution of which is straightforward. In the second step the dummy variable is replaced by its defining derivative and the resulting equation is integrated again, to yield:

$$T_1 = \frac{1}{\kappa_{11}}\left\{g_{11}\tan\left[\frac{g_{11}}{2}(\eta_1 + g_{12})\right] - \kappa_{12}\right\} \quad (12)$$

where g_{11} and g_{12} are the integration coefficients in region [1]. It follows from Eq. (12) that $k_{11} \neq 0$ implying that the specific heat may not be constant in region [1]. Substitution of boundary condition (8) into Eq. (12) yields the functional relationship between g_{12} and g_{11}. This leaves only one integration coefficient, g_{11}, in the expression for T_1:

$$T_1 = \frac{1}{\kappa_{11}}\left[g_{11}\frac{(\kappa_{11}T_{ml} + \kappa_{12}) + g_{11}\tan(g_{11}\eta_1/2)}{g_{11} - (\kappa_{11}T_{ml} + \kappa_{12})\tan(g_{11}\eta_1/2)} - \kappa_{12}\right] \quad (13)$$

The remaining boundary condition, Eq. (9), is now used to obtain an implicit expression for coefficient g_{11}:

$$k_l D\left(T_{ml} - T_b - \frac{\dot{q}_{\text{met}}}{\dot{w}_b C_b}\right) = \frac{k_1 g_{11}^2}{2\kappa_{11}}\sec^2\left[\tan^{-1}\left(\frac{\kappa_{11}T_{ml} + \kappa_{12}}{g_{11}}\right)\right] \quad (14)$$

A similar procedure is applied to region [2] for a coordinate system located on isotherm T_{m1}. The resulting temperature distribution in region [2], using boundary condition (8), is given by:

$$T_2 = \frac{1}{\kappa_{21}}\left[g_{21}\frac{(\kappa_{21}T_{m1} + \kappa_{22}) + g_{21}\tanh(-g_{21}\eta_2/2)}{g_{21} + (\kappa_{21}T_{m1} + \kappa_{22})\tanh(-g_{21}\eta_2/2)} - \kappa_{22}\right] \quad (15)$$

where g_{21} is given by the implicit expression which was obtained by substitution of Eq. (9) into Eq. (15):

$$\frac{k_1 g_{11}^2}{\kappa_{11}}\sec^2\left[\tan^{-1}\left(\frac{\kappa_{11}T_{m1} + \kappa_{12}}{g_{11}}\right)\right] = -\frac{k_2 g_{21}^2}{\kappa_{21}}\operatorname{sech}^2\left[\tanh^{-1}\left(\frac{\kappa_{21}T_{m1} + \kappa_{22}}{g_{21}}\right)\right] \quad (16)$$

The frozen region, [f], is treated next to complete the computation procedure for the quasi-steady state. It is noted that the specific heat in this region is constant and thus $\kappa_{f1} = 0$. Upon integration of Eq. (10), using boundary conditions (8) and (9),

Table 1 Typical thermophysical properties of a peripheral biological tissue; data compiled from Chato (1985)

Initial Temperature, °C	37
Blood Temperature, °C	37
Thermal Conductivity in the unfrozen region W/m°C	0.5
Thermal Conductivity in region [1], W/m°C	1.7
Thermal Conductivity in region [2], W/m°C	1.9
Thermal Conductivity in the frozen region, W/m°C	2.0
Volumetric Specific Heat in the unfrozen region, MJ/m³ °C	3.6
Volumetric Specific Heat in the frozen region, MJ/m³ °C	1.8
Latent Heat of solidification, MJ/m³	233.4
Volumetric Specific Heat Source of Blood, $\dot{w}_b C_b$, kW/m³ °C	2.5
Metabolic Heat Generation, kW/m³	2.5

an explicit temperature distribution for the frozen region is obtained:

$$T_f = \frac{k_2}{k_f}\frac{g_{21}^2}{2\kappa_{f2}\kappa_{21}}\,\mathrm{sech}^2\left[\tanh^{-1}\left(\frac{\kappa_{21}T_{mf}+\kappa_{22}}{g_{21}}\right)\right] \times [1-\exp(\kappa_{f2}\eta_f)] + T_{mf} \quad (17)$$

We now turn to finding the boundary condition, or the forcing function, at the interface between the cryoprobe and the phase changing medium. This boundary condition may be visualized as the temperature variations obtained by an observer moving at a constant velocity from $+\infty$ in the $-x$ direction relative to the quasi-steady-state solution. The boundary condition obtained by this method is precise but is impractical since infinite time is required to travel from $x = \infty$ to $x = 0$. We, therefore, turn to seeking an approximate solution to the forcing function at $x = 0$.

It is first noted that the temperature distribution in the unfrozen region decays exponentially to a constant value, Fig. 2. We can now place the observer, who is moving at a constant velocity in the negative x direction, on point x_0. The location of this point can be selected such that the exponential in Eq. (2) would be of an arbitrarily small value, ϵ:

$$\epsilon = \exp(-Dx_0) \quad (18)$$

This amounts to replacing the uniform initial condition with an exponential condition. The maximal difference between these two conditions appears at the interface between the cryoprobe and the phase changing medium. The new approximate boundary condition, at the interface between the cryoprobe and the tissue, may now be expressed by:

$$T_t(0,t) = \left(T_b + \frac{\dot{q}_{\mathrm{met}}}{\dot{w}_b C_b}\right)\cdot[1-\epsilon\exp(-D\dot{s}t)] + \epsilon T_{ml}\exp(-D\dot{s}t) \quad (19)$$

As discussed above, under quasi-steady state, wherein all freezing fronts are moving at a constant and identical velocity, the cooling rates on these fronts would also be invariable. This condition of fixed cooling rates at the freezing fronts is actually the desired Stefan's condition (1891). These cooling rates may now be evaluated by an inverse transformation from coordinate system ξ back to x:

$$\frac{\partial T_t}{\partial t}(x,t) = \frac{\partial T_t}{\partial t}(\xi,t) - \dot{s}\frac{\partial T_t}{\partial \xi}(\xi,t) \quad (20)$$

Since in the coordinate system ξ the medium is in a quasi-steady state, the cooling rate at the front s_t, as viewed from the unfrozen region, is given by:

$$\frac{\partial T_t}{\partial t}(s_t,t) = -\dot{s}\frac{dT_t}{d\xi}(\xi=0) = \dot{s}D\left(T_{ml} - T_b - \frac{\dot{q}_{\mathrm{met}}}{\dot{w}_b C_b}\right) \quad (21)$$

By equating heat fluxes at both sides of freezing front s_t, the cooling rate, as viewed from the freezing region [1], is given by:

$$\frac{\partial T_1}{\partial t}(s_t,t) = \frac{k_t}{k_1}\frac{\partial T_t}{\partial t}(s_t,t) \quad (22)$$

Similar mathematical derivations may be applied at freezing fronts s_1 and s_f. This involves differentiation of the temperature distributions at the origins of the coordinate systems and equating the heat fluxes on both sides of each front. Since this method involves an iterative process of calculation of coefficients, an alternative integral procedure is proposed. This procedure allows the calculation of the cooling rates at the freezing fronts s_1 and s_f, based on the cooling rate at front s_t, Eq. (21).

We first define a control volume encompassing regions [1] and [2] in which phase change is occurring. In a quasi-steady state, the difference between the incoming and outgoing heat fluxes equals the change in enthalpy in the control volume:

$$\left(-k_t\frac{\partial T}{\partial x}\bigg|_{x=s_t}^{+}\right) - \left(-k_f\frac{\partial T}{\partial x}\bigg|_{x=s_f}^{-}\right) = (h|_{x=s_t} - h|_{x=s_f})\frac{ds}{dt} \quad (23)$$

where the superscripts $(+)$ and $(-)$ indicate calculation by the unfrozen and frozen regions, respectively. It is noted that the change in enthalpy inside the control volume due to sensible heat is about two orders of magnitude smaller than that due to latent heat. Thus, as a first approximation, the change in enthalpy may be taken as the latent heat of freezing. With this approximation and coordinate transformation in Eq. (23), substitution into Eq. (20) yields the cooling rate as viewed from the frozen region:

$$\frac{\partial T}{\partial t}\bigg|_{x=s_f}^{-} = \dot{s}\frac{dT}{d\eta_2}\bigg|_{\eta_2=0} = -\frac{k_t\dot{s}}{k_f}\frac{dT}{d\xi}\bigg|_{\xi=0} - \frac{\dot{s}^2}{k_f}(h|_{x=s_t} - h|_{x=s_f}) \cong \frac{k_t}{k_f}\frac{\partial T}{\partial t}\bigg|_{x=s_t}^{+} - \frac{\dot{s}^2 L}{k_f} \quad (24)$$

As noted above, the rate of change of temperature on s_f, viewed from region [2], is equal to the product of the change given by Eq. (24) and the ratio of thermal conductivities of region [2] and of the frozen region. Equation (24) reveals that, with the increase of the freezing front velocity, the cooling rate in the frozen region would also increase.

Results and Discussion

The present solution is compared to an existing analytic solution to an inverse-Stefan problem in a pure material (Rubinsky and Shitzer, 1976). In this solution phase change is assumed to occur at a single temperature at which the thermophysical properties are assumed to change stepwise. Unlike the present solution, the previous one assumes that the entire latent heat of freezing is absorbed at the single freezing front. The two solutions are in complete agreement in the unfrozen region. Therefore, com-

Table 2 Phase-change interface temperatures, in °C, used for the comparison of the present solution with an existing one of a pure material (Rubinsky and Shitzer, 1976)

	$T_{m\ell}$	T_{m1}	T_{mf}
ΔT_1	-1.0	-1.05	-1.1
ΔT_2	-1.0	-1.5	-2.0
ΔT_3	-1.0	-3.0	-5.0
ΔT_4	-1.0	-3.0	-8.0

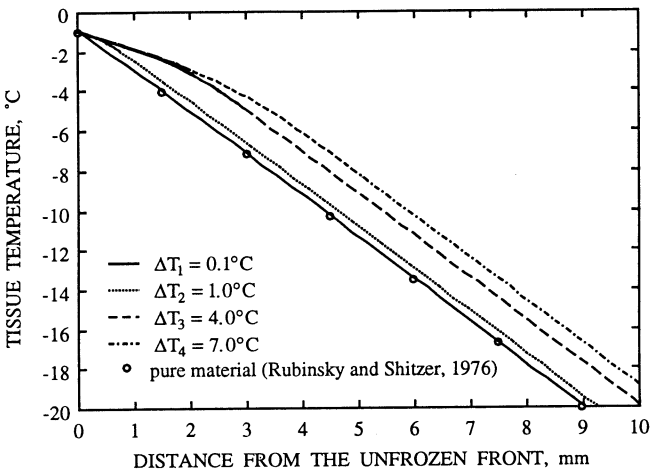

Fig. 3 Comparison of a solution to an inverse-Stefan problem in a biological tissue behaving like a pure material (Rubinsky and Shitzer, 1976) with the present solution of a nonideal biological tissue. Parameter values are presented in Table 1

parison is carried out in the frozen region and in the regions undergoing phase change. For comparison purposes we assume thermophysical properties typical to peripheral biological tissues, Table 1.

Comparison is presented for four cases differing in the temperature range in which phase change occurs, Table 2 and Fig. 3. The first case depicts a freezing process in pure materials in which phase change occurs at a single temperature. The second case depicts a real material that differs only slightly from a pure material. The third and fourth cases simulate typical biological materials in which phase change occurs gradually over a range of temperatures. These latter two cases demonstrate, among other things, the uncertainty relating to the precise temperatures that define the phase-change range. Thus, it is common to assume that peak phase change in a biological medium occurs at −3°C. The lower temperature bound, on the other hand, is less certain and ranges between −5°C and −8°C (Altman and Dittmer, 1971; Wessling and Blackshear, 1973).

Figure 3 shows the similarity in the temperature distributions in the frozen region for all cases studied. This similarity is retained even in the fourth case wherein an asymmetric specific heat function was assumed. Practically, all four temperature distributions may be considered to be identical following adjustments of the different temperature ranges in which phase change occurs. This similarity of solutions could be expected since the resulting temperature distributions in the phase-changing range are functionally dependent on the specific heat. Figure 3 indicates, clearly, that the various cases evaluated by the present solution conform closer to the existing solution as the phase-change temperature range is narrowed down.

The functional behavior of the solution coefficients, g_{11} and g_{21}, is discussed next. These coefficients are obtained, through an iterative process, by Eqs. (14) and (16) for regions [1] and [2], respectively. It is noted that although the solutions, as presented by Eqs. (13) and (15), are straightforward, their actual computation requires the values of the g_{i1} coefficients. These are obtainable by a trial and error process. Results for g_{11} are presented graphically in Fig. 4 by means of the following two coefficients:

$$a_1 \equiv 2\kappa_{11}\frac{k_\ell}{k_1}D\left(T_{ml} - T_b - \frac{\dot{q}_{\text{met}}}{\dot{w}_b C_b}\right) \tag{25}$$

$$b_1 \equiv \kappa_{11}T_{ml} + \kappa_{12} \tag{26}$$

It is noted that for fixed values of the coefficient b_1, there is a similarity in the behavior of g_{11} over a wide range of physiologically relevant values. At large values of the coefficient a_1, values of g_{11} converge asymptotically to the same function, and become independent of b_1, Fig. 4.

Coefficients g_{21} are presented in Fig. 5. Here, too, we define two new coefficients to facilitate the graphic presentation of g_{21}:

$$a_2 \equiv -\frac{\kappa_{21}k_1 g_{11}^2}{\kappa_{11}k_2}\sec^2\left[\tan^{-1}\left(\frac{\kappa_{11}T_{m1} + \kappa_{12}}{g_{11}}\right)\right] \tag{27}$$

$$b_2 \equiv \kappa_{21}T_{m1} + \kappa_{22} \tag{28}$$

It is seen that for a range of low values of a_2 and for $b_2 > 0$, g_{21} assumes constant values, which are dependent on b_2. At high values of a_2, g_{21} converges to a log-linear function, independent of b_2, Fig. 5.

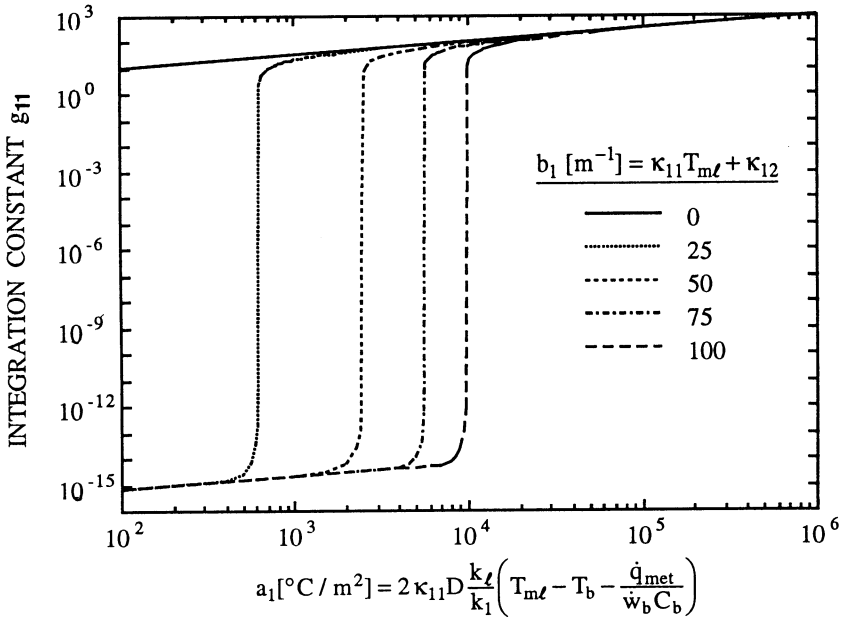

Fig. 4 Computed values of the integration constant g_{11}, Eq. (14), versus the coefficients a_1 and b_1, defined by Eqs. (25) and (26), respectively

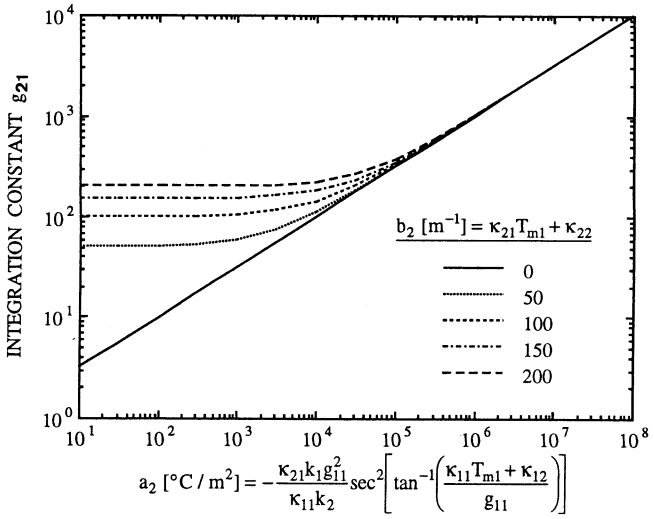

Fig. 5 Computed values of the integration constant g_{21}, Eq. (16), versus the coefficients a_2 and b_2, defined by Eqs. (27) and (28), respectively

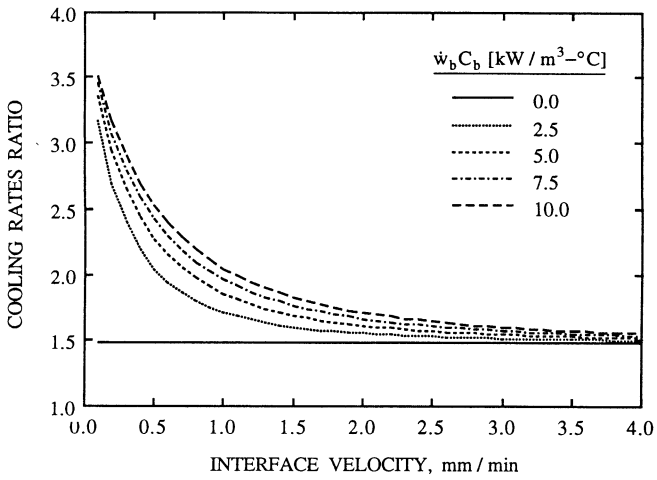

Fig. 7 Cooling rates ratio of the unfrozen to frozen region at the freezing fronts versus the interface velocity

We now turn to the cryosurgical process. In this study it is assumed that enhanced success of this process may be achieved by maintaining a prespecified cooling rate on the freezing front. In this case the freezing rates of interest are those existing at fronts s_f and s_l, as calculated in the frozen and unfrozen regions, respectively. Figure 6 shows the relationship between the velocity of propagation and the cooling rate at freezing front s_f. It is seen that these two parameters are exponentially dependent for a case of zero blood flow. As blood perfusion increases, acting essentially as a heat source in the medium, cooling rate must also increase to maintain any desired constant velocity of propagation of the freezing front.

The relationship between cooling rate ratio and the velocity of propagation of freezing fronts is shown in Fig. 7. The cooling rate ratio is taken as the one between the unfrozen and frozen regions, as viewed from those regions, respectively. It is seen that as the velocity of propagation increases, the effect of blood perfusion on the cooling rate ratio diminishes. Actually, at very high velocities of propagation of the freezing front, which may not be attainable in practice, the cooling rate ratio equals that of the in-vitro case of no blood flow. As can be seen from Eq. (24), the cooling rate ratio depends linearly on the thermal conductivity ratio and on the enthalpy changes. The thermal conductivity values in the frozen and unfrozen regions bound the values in regions [1] and [2] while the enthalpy changes monotonically with temperature across these regions. Thus, the cooling rates within the regions undergoing phase change are between the cooling rates at the frozen and the unfrozen interfaces.

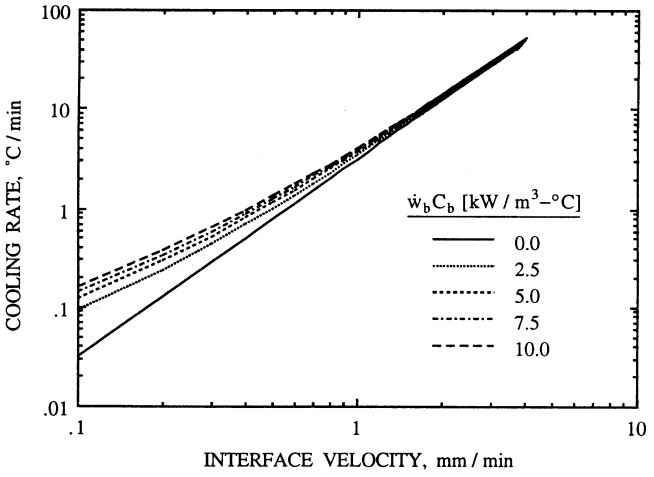

Fig. 6 Cooling rate at the freezing front s_f as viewed from the frozen region, versus the freezing front velocity

The forcing function solution of the inverse-Stefan problem is studied next. This function is evaluated for five cases of various combinations of metabolic heat generation and specific heat source of the blood, Table 3, and for thermophysical properties listed in Table 1. A freezing rate of 10°C/min was assumed in the frozen region at the freezing front, which leads to freezing fronts velocities of about 1.6 mm/min, as can be seen in Fig. 6.

The expression for the forcing function for the condition in which the unfrozen region is in contact with the cryoprobe was obtained by Eq. (19), using an initial parameter value of $\epsilon = 0.05$. The forcing functions relating to regions [1] and [2] were calculated next, by replacing η_1 and η_2 with $\dot{s}t$, in Eqs. (13) and (15), respectively. The integration constants g_{11} and g_{21} were evaluated from Eqs. (14) and (16), as presented in Figs. 4 and 5, respectively. It is noted that for typical thermophysical properties of biological tissues and for cooling rates above 4°C/min in the frozen region at the freezing front, the integration constants g_{11} and g_{21} are almost log-linearly dependent on a_1 and a_2, respectively, and are independent of b_1 and b_2. These simplified relations are: $g_{i1} = a_i^{1/2}$. The forcing function relating to the frozen region was calculated last by a similar procedure, replacing η_f with $\dot{s}t$ in Eq. (17), following the formation of all of the freezing fronts. The liquid nitrogen boiling temperature, −196°C, was taken as the lowest temperature bound of the forcing functions.

The results obtained for the forcing functions for the five cases studied, for a cooling rate of 10°C/min at s_f, are presented in Fig.

Table 3 Duration and depth of penetration of cryotreatments, for a cooling rate of 10°C/min at the frozen front s_f, for five cases of various combinations of metabolic heat generation and specific heat source of the blood

Case No.	$\dot{w}_bC_b$ kW/m^3-°C	$\dot{q}_{met}$ kW/m^3	Duration of cryotreatment, min	Depth of freezing penetration - s_f front, mm	Phase transition width (regions [1] and [2], mm
1	0.0	0.0	37.1	40.1	3.8
2	5.0	0.0	32.7	36.7	2.9
3	5.0	10.0	32.1	35.8	2.8
4	10.0	0.0	30.1	34.5	2.5
5	10.0	10.0	29.8	34.1	2.4

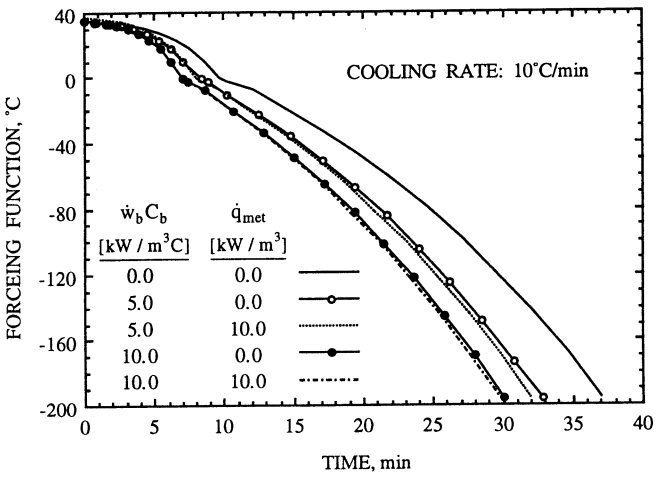

Fig. 8 Forcing functions of the inverse-Stefan problem for various combinations of heat sources and a cooling rate of 10°C/min at the frozen front s_f. Parameter values are presented in Tables 1 and 3.

8. Numerical results of the duration of the cryotreatment, depth, and freezing penetration (defined by s_f), and the phase transition width (defined by the distance between the freezing fronts s_l and s_f) are all presented in Table 3. It is seen that the dependence of the forcing function on the relatively high metabolic heat generation, with respect to blood perfusion, is relatively weak. It can also be seen that with the increasing of blood perfusion, the slope of the forcing function increases, the depth of freezing penetration decreases, and the phase transition widens. Maximal blood perfusion and metabolic heat generation (Case 5) reduce the duration of cryotreatment by 20 percent, reduce the depth of freezing penetration by 15 percent, and reduce the phase transition width by 37 percent, all with respect to a tissue devoid of heat sources (Case 1).

The proposed exact solution of the inverse Stefan problem is one dimensional and is presented for Cartesian coordinates. It can be shown mathematically that a solution to the multidimensional inverse Stefan problem may not exist except for unique cases. However, observing that cell destruction increases with the decreasing of the freezing rates, in the range of low freezing rates, the present solution can be used as an upper bound forcing function for the multidimensional problem. By applying the proposed forcing function solution to a multidimensional cryotreatment one can ensure that the actual freezing rates would be equal to, or lower than, the defined freezing rate of the one-dimensional solution at all times. It can be expected that in superficial cryotreatments, and in cases of low depth of freezing penetration with respect to a typical cryoprobe dimension, the one-dimensional case will be close to the multidimensional one. Accordingly, the depth of freezing penetration in the one-dimensional case can be taken as the maximal bound for the multidimensional case.

Conclusion

An analytic solution to the inverse-Stefan problem in a biological tissue, in which a constant cooling rate is maintained at the freezing front, is presented. The solution is derived for a nonideal material and is based on the enthalpy method applied in the range of phase-change temperatures. Thermal effects of blood perfusion as well as metabolic heat and density changes are accounted for. Results are compared to an existing solution derived for a pure material. The comparison was facilitated by assuming that phase change occurs over a very narrow temperature range, essentially simulating the behavior of a pure material. Conformity of the results of the two solutions is very good.

The solution is studied for a range of parameters, which are applicable to biological tissues undergoing cryosurgical processes. The relationship between the velocity of propagation of the freezing front and the constant cooling rates maintained at the freezing fronts is presented graphically. Results indicate the possibility to control the cooling rate at the freezing front for a range of phase-change temperatures, thermophysical and physiological properties and parameters.

Acknowledgments

This work was supported in part by the James H. Belfer Chair in Mechanical Engineering and by the Technion Vice President for Research Fund, Sam Rose Research Fund.

References

Akhtar, T., Pegg, D. E., and Foreman, J., 1979, "The Effect of Cooling and Warming Rates on the Survival of Cryopreserved L-Cells," *Cryobiology,* Vol. 16, pp. 424–429.

Alexiades, V., and Solomon, A. D., 1993, *Mathematical Modeling of Melting and Freezing Processes,* Hemisphere Publishing Corporation, Washington, DC.

Altman, P. L., and Dittmer, D. S., 1971, *Respiration and Circulation,* Federation of American Societies for Experimental Biology (Data Handbook), Bethesda, MD.

Augustynowicz, S. D., and Gage, A. A., 1985, "Temperature and Cooling Rate Variations During Cryosurgical Probe Testing," *International Journal of Refrigeration,* Vol. 8, No. 4, pp. 198–208.

Budman, H. M., Shitzer, A., and Dayan, J., 1995, "Analysis of the Inverse Problem of Freezing and Thawing of a Binary Solution During Cryosurgical Processes," ASME *Journal of Biomechanical Engineering,* in press.

Carslaw, H., and Jaeger, J., 1959, *Conduction of Heat in Solids,* Oxford, Chap. 11, pp. 282–286.

Chato, J. C., 1985, "Selected Thermophysical Properties of Biological Materials," in: *Heat Transfer in Medicine and Biology,* A. Shitzer and R. C. Eberhart, eds., Plenum Press, New York, Vol. 2, pp. 413–418.

Fahy, G. M., 1981, "Analysis of Solution Effect Injury: Cooling Rate Dependence of the Functional and Morphological Sequellae of Freezing in Rabbit Renal Cortex Protected With Dimethyl Sulfoxide," *Cryobiology,* Vol. 18, pp. 550–570.

Farrant, J., 1971, "Cryobiology: The Basis of Cryosurgery," in: *Cryogenics in Surgery,* H. von Leden and W. G. Cahan, eds., Lewis, London, pp. 15–42.

Gage, A. A., Guest, K., Montes, M., Caruna, J. A., and Whalen, D. A., Jr., 1985, "Effect of Varying Freezing and Thawing Rates in Experimental Cryosurgery," *Cryobiology,* Vol. 22, pp. 175–182.

Goodman, T. R., 1958, "The Heat Balance Integral and Its Application to Problems Involving a Change of Phase," *Transactions of the ASME,* Vol. 80, pp. 335–342.

McGrath, J. J., 1993, "Low Temperature Injury Processes," in: *Advances in Bioheat and Mass Transfer,* ASME HTD-Vol. 268, pp. 125–132.

Mazur, P., 1963, "Kinetics of Water Loss From Cells at Subzero Temperatures and the Likelihood of Intracellular Freezing," *The Journal of General Physiology,* Vol. 47, pp. 347–369.

Mazur, P., Leibo, S., and Chu, E. H. Y., 1972, "A Two-Factor Hypothesis of Freezing Injury," *Experimental Cell Research,* Vol. 71, pp. 345–355.

Miller, R. H., and Mazur, P., 1976, "Survival of Frozen-Thawed Human Red Cells as a Function of Cooling and Warming Velocities," *Cryobiology,* Vol. 13, pp. 404–414.

Orpwood, R. D., 1981, "Biophysical and Engineering Aspects of Cryosurgery," *Physical and Medical Biology,* Vol. 26, No. 4, pp. 555–575.

Pennes, H. H., 1948, "Analysis of Tissue and Arterial Blood Temperature in the Resting Human Forearm," *Journal of Applied Physiology,* Vol. 1, pp. 93–122.

Rubinsky, B., and Shitzer, A., 1976, "Analysis of a Stefan-Like Problem in a Biological Tissue Around a Cryosurgical Probe," ASME JOURNAL OF HEAT TRANSFER, Vol. 98, pp. 514–519.

Rubinsky, B., and Onik, G., 1991, "Cryosurgery: Advances in the Application of Low Temperatures to Medicine," *International Journal of Refrigeration,* Vol. 14, pp. 190–199.

Stefan, J., 1891, "Über die Theorie der Eisbildung, Insbesondere über die Eisbildung in Polarmeere," *Annals Physical Chemistry,* Vol. 42, pp. 269–286.

Voller, V. R., 1986, "A Heat Balance Integral Based on the Enthalpy Formulation," *International Journal of Heat and Mass Transfer,* Vol. 30, pp. 604–606.

Wessling, F. C., and Blackshear, P. L., 1973, "The Thermal Properties of Human Blood During the Freezing Process," ASME JOURNAL OF HEAT TRANSFER, Vol. 95, pp. 246–249.